Microelectronic Engineering 121 (2014) 87–91

Contents lists available at ScienceDirect

Microelectronic Engineering

journal homepage: www.elsevier.com/locate/mee

FIB patterning of dielectric, metallized and graphene membranes: A comparative study

A. Hemamouche [a], A. Morin [a], E. Bourhis [a], B. Toury [b], E. Tarnaud [c], J. Mathé [c], P. Guégan [g], A. Madouri [a], X. Lafosse [a], C. Ulysse [a], S. Guilet [a], G. Patriarche [a], L. Auvray [d], F. Montel [d], Q. Wilmart [e], B. Plaçais [e], J. Yates [f], J. Gierak [a,*]

[a] LPN-CNRS, Route de Nozay, 91460 Marcoussis, France
[b] Laboratoire des Multimatériaux et Interfaces – UMR 5615, Univ. Claude Bernard Lyon1, 69100 Villeurbanne, France
[c] LAMBE-CNRS-UEVE-CEA, Univ. d'Evry-Val-d'Essonne, France
[d] Matière et Systèmes Complexes, UMR 7057, Paris Diderot University, France
[e] Laboratoire Pierre Aigrain, Département de Physique de l'ENS, 24, rue Lhomond, 75005 Paris, France
[f] Laboratory of Single Molecule Processes, ITQB-UNL, Av. da República, 2780-157 Oeiras, Portugal
[g] Laboratoire de Chimie des Polymères - UMR 7610, UPMC3, rue Galilée, 94200 Ivry sur Seine, France

ARTICLE INFO

Article history:
Received 22 October 2013
Received in revised form 7 March 2014
Accepted 22 March 2014
Available online 3 April 2014

Keywords:
FIB
Ultra-thin membranes
Dielectric films
Graphene
Nanopores
Boron nitride

ABSTRACT

Fabrication of nanopores and nanomasks has recently emerged as an area of considerable interest for research applications ranging from optics, to electronics and to biophysics. In this work we evaluate and compare the fabrication of nanopores, using a finely focused gallium beam, in free-standing membranes/films made of Si, SiN, and SiO_2 (having thicknesses of a few tens of nanometers) and also in graphene and hexagonal boron nitride (h-BN) atomically thin suspended sheets. Mechanical resistance, charging effects and patterning performances are evaluated and compared. In spite of the very different properties of the membranes we report that reproducible nanopore fabrication in the sub-10 nm range can be achieved in both amorphous and atomically thin sheets using Ga^+ focused ion beams (FIB).

© 2014 Elsevier B.V. All rights reserved.

1. Introduction

Nanofabrication with focused ion beams (FIB) has emerged in recent years as a technique of choice for producing nanostructures. Gallium ion beams, with landing energies in the 30–50 keV range were found to be well suited to nano-fabrication because they suffer very little scattering and therefore allow very localized surface modifications. However, since the FIB patterning technique relies on sequential processing, it is much slower than parallel processing via optical or e-beam lithography [1,2] and does not meet mass-production capability levels. As a consequence, FIB technology has found some market niches such as in Integrated Circuits (IC) manufacture as a complement to other technologies; for relatively small operations on individual chips within wafers. Examples include failure analysis and IC testing [3]. Nevertheless one must keep in mind that FIB technology is highly flexible and allows for direct and local surface modifications to be made, with dimensions that are characteristic of nanoscience. One important challenge for nanosciences related to the fabrication of nanopores in solid-state materials; nanopores that have dimensional stability, precise diameters and channel lengths, adjustable surface properties and the potential for integration into devices. Various routes have been explored to meet the challenge of fabricating pores with true nanometer dimensions. Using techniques developed for Si-based microfabrication, free-standing membranes of Si, SiN, or SiO_2 can be fabricated [4] and are commercially available [5]. For patterning nanosized holes in these materials, a high density electron-beam, generated within a transmission electron microscope (TEM), is generally used [6,7]. This process of glassmaking at the nanoscale allows for the fabrication of stable pores, but requires irradiation times from a few minutes to half an hour. In addition, the necessity to conduct this process inside a TEM requires a specific chip size (3 mm diameter in most cases) to be used and only one nanopore can be fabricated at a time under the permanent supervision of an operator. Therefore TEM patterning process of nanopores remains a laborious process, is limited in terms of production and not suitable for commercial fabrication. Nanopore

* Corresponding author. Tel.: +33 1 69 63 60 75; fax: +33 1 69 63 60 06.
E-mail address: jacques.gierak@lpn.cnrs.fr (J. Gierak).

http://dx.doi.org/10.1016/j.mee.2014.03.020
0167-9317/© 2014 Elsevier B.V. All rights reserved.

fabrication is a perfect demonstration of the difficulties faced when developing an innovative process suitable for niche products and new markets. Several routes are also explored such as Helium ions used to pattern nanopores [8], as well as cold ion beam sculpting techniques [9], direct focused ion beam approach with back face particle detection [10] and finally ion tracks that are created when high-energetic heavy ions with energy of about 1 MeV/nucleon [11].

Some time ago, in order to explore the ultimate patterning potential of a focused ion beam, we proposed to develop and build a specific, dedicated FIB nanowriter capable of tackling such nanotechnology challenges [12]. The principle was to direct a highly focused pencil of selected gallium ions onto a sample surface in order to take advantage of locally induced modifications. Sample positioning using the highest metrological standards in terms of positioning and of ion counting was foreseen to allow unattended or batch processing; a new functionality for FIB technology. Using this machine, we have already demonstrated that nanofabrication using FIB allows for the fabrication of a small series, or the customization of individual nanopore-based devices in dielectric or metallized membranes. With the advent of atomically-thin graphene and of hexagonal boron nitride (h-BN) we were interested in performing a comparative study; to assess the respective limits of both the materials and the processes.

2. Experimental

FIB nano-engraving of a membrane is of particular interest if the membrane is homogeneous, conductive and as thin as possible; i.e. with a thickness comparable to, or less than the projected range of the incoming ions. In our case, as already shown elsewhere [13], for nanometer-scaled nanopore engraving, a target media with a maximum thickness of 20 nm is preferable. At the same time, very important differences in engraving performances and resolution can be observed between crystalline materials and polycrystalline media. For this comparative study we have selected thin, Si-based materials including SiN, SiC and SiO_2 membranes [5]. Atomically thin sheets of exfoliated graphene and hexagonal boron nitride (h-BN), as well as graphene produced by chemical vapor deposition (CVD) are also used as target materials.

2.1. SiN, SiO_2, Si

- Arrays of nanopores for ion doses and size calibration. As described elsewhere we began by fabricating [13] arrays of nanopores, drilled with increasing FIB dosage, to calibrate the critical dwell time required to define open nanopores (Fig. 1).
- Single nanopore. Fabricating and localizing a single nm-sized pore requires the implementation of precise metrology and reference marks. Thanks to our precise sample positioning capability (2 nm), we used a method developed several years ago by our team allowing for a "low-dose marking process" and higher dose nanopore drilling to be carried out in the same run (Fig. 2) [14]. To achieve successful fabrication of nanopores in Si-based thin membranes, a first requirement is to select membranes that are planar to keep a constant focus distance for our highly demagnified FIB optics, and low stressed in order to resist the mechanical stress resulting from modifications induced by the ion beam patterning. Fabricating the smallest possible nanopores in Si-based thin windows raises further experimental requirements. The first relates to the variation of membrane thickness within a single batch (i.e. within a 2–5 inch wafer), making precise dose calibration difficult. Indeed we systematically obtain narrow pores using a variable dose matrix, with small increments in dwell-time, which is difficult to reproduce for single pores. For single pores a safety margin is employed resulting in slightly larger ion doses and therefore pore diameters. A second observation is that when using a narrowly focused Ga-FIB (30–35 keV), the membrane grain size governs the minimum obtainable pore diameter. Nanometer sized-grains in the Si-based polycrystalline film leaded to the fabrication of pores in the 2–5 nm scale in our experience (FIB probe 5 nm Full Width at Half Maximum). Smaller or larger grain sizes resulted in pore sizes of or around 10 nm. Finally, materials with high secondary electron emission allow for highly contrasted images to be obtained in the Scanning Ion Microscopy (SIM) mode and therefore much more precise FIB probe focus and shaping. Indeed low contrasted images were found to be very limiting for the engraving of nanopores in these highly insulating Si-based materials.

2.2. Graphene

Graphene is a strictly two-dimensional hexagonal lattice of carbon atoms with a thickness of one or a few atomic layers [15]. The motivation for our study arose from the observation that isolated atomically thin conducting membranes of graphene can be used for carving nanopores and these can be used to characterize single molecules of DNA in ionic solution [16]. Indeed when immersed in an ionic solution, a layer of graphene becomes a new electrochemical structure, having properties that are the consequence of the atomic-scale proximity of its two opposing liquid–solid interfaces. Preparation and peeling of Highly Oriented Pyrolytic Graphite (HOPG) flakes was achieved by mechanical exfoliation from natural HOPG as described elsewhere [17]. Flakes were exfoliated first

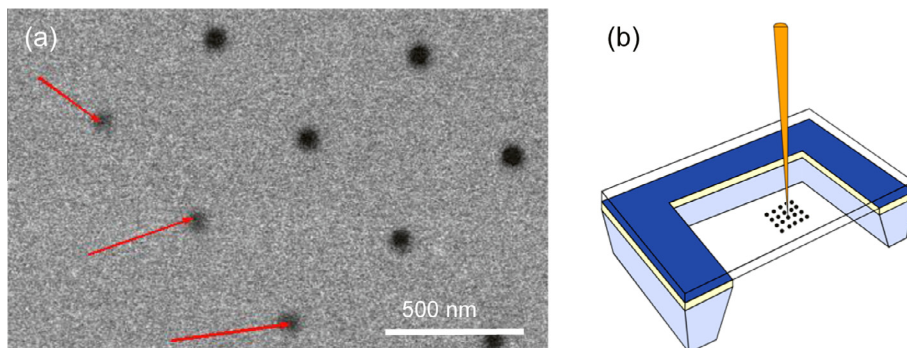

Fig. 1. (a) Array of nanopores drilled with increasing FIB doses used to calibrate the critical dwell time defining open nanopores. Low energy SEM imaging reveals sub-5 nm openings (red arrows) in agreement with the SiO_2 membrane grain size and roughness. (b) Schematic of the nanopore array engraving. (For interpretation of the references to colour in this figure legend, the reader is referred to the web version of this article.)

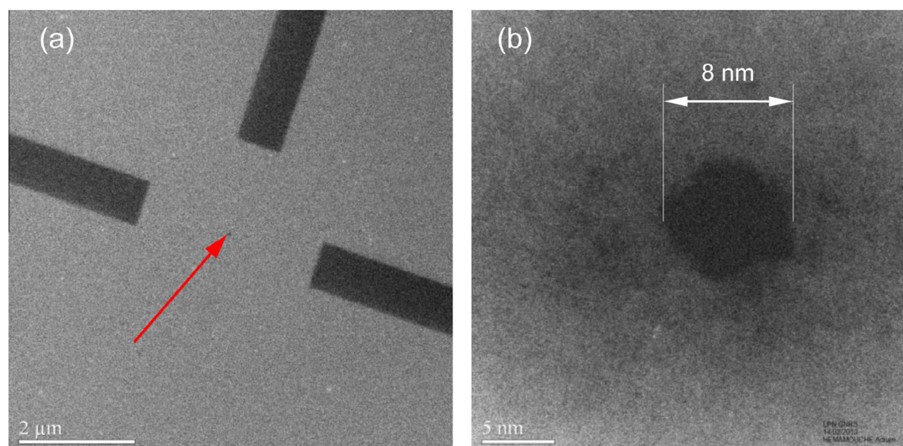

Fig. 2. (a) TEM image of a single nanopore aligned with low dose markers added for localization pore ~10^5/pt; marker 10^2/cm^2) in a single FIB patterning sequence with nm-sized metrology. (b) Detail of a fabricated 8 nm spherical nanopore.

over a 270 nm thick SiO_2 layer covering the silicon substrate. The deposited graphene flakes were then peeled and their thickness reduction meticulously inspected and monitored using optical and AFM microscopy. The final transfer of the graphene sheets was performed over different samples. (i) Holey films onto copper grids available from Agar Scientific and (ii) FIB-drilled Si-based window chips using the wedging method described elsewhere [18].

2.2.1. Exfoliated graphene flakes from HOPG

For this application, aimed at producing bio-sensing devices, micro-sized pores were first FIB-patterned onto SiNx chips prior to the transfer of the graphene flakes. Since a positioning accuracy at the micrometer scale is required, we developed a method consisting of locking a precisely identified graphene flake into a transparent media (millimeter-scaled resist drop) and then used this media to manipulate and position the flake over the hole in the SiNx chip. This operation is achieved via the intercalation of a water layer in between the substrate and the hydrophobic locking media i.e. polymethyl methacrylate (PMMA) or a solution of cellulose acetate butyrate (CAB 30 mg/ml) dissolved in ethyl acetate. After flake placement, the locking media was dissolved leaving the graphene flake across the µm-sized hole in the SiN membrane. As a final nanofabrication step we have used our high resolution FIB nanowriter, that is described in detail elsewhere [19], for patterning the nanopores in the graphene flake. This setup for holding the graphene was found to be very suitable and allowed for precise placement of the nanopore and FIB performance control. Indeed for a high resolution FIB machine, working in strong demagnification mode, the working distance (WD) must be controlled within a few tens of µm to keep the probe focus in between the Gauss plane and the "disk of least confusion". Using alignment marks defined during the initial µm-aperture engraving in the SiN membrane, an accurate pore placement was made possible. The Scanning Ion Microscopy image was used in the calibration phase to check the thickness of the films. Indeed for thicknesses larger than ~10 atomic layers (3 nm) a graphene membrane is not transparent to the 30 keV gallium ions (Fig. 3a). Indeed almost no gallium ions are transmitted with sufficient energy to induce a secondary electron signal (SE) from impacting the aluminium sample holder underneath. Graphene membranes were found to be extremely resistant to ion bombardment, to resist ion microscopy imaging and no surface charging was observed; this allowed for precise focusing and probe shaping. Furthermore, the excellent thickness uniformity of exfoliated graphene flakes allows for almost perfect dwell-time calibrations on test samples deposited onto holey films [20] (Fig. 3a).

2.2.2. Chemical vapor deposited graphene films

Graphene membranes were prepared by a CVD method using a home-built thermal system where copper foil was used as the catalytic substrate for graphene growth. During graphene growth, the temperature was held constant at 1040 °C and a mixture of propane gas combined with argon, hydrogen, and helium gas is used as feed-stock. Once the graphene/copper foil was cooled and removed from the furnace, a polymer (PMMA), was spin-coated onto the graphene as a support to aid the transfer of graphene to specific substrates. The samples were subsequently soaked in a copper etchant consisting of ammonium persulfate until the polymer/graphene film was cleanly separated from the copper. The films were then cleaned in deionized-water followed by transfer on to either holey films for calibration or onto micro-fabricated holes (Fig. 4a).

The main advantage of using CVD graphene films is that millimeter sized films can easily be obtained and could be transferred onto our test devices. Unfortunately at this moment the minimum film thickness seems to be larger, than exfoliated HOPG flakes, an artifact that possibly derives from contamination effects induced by the PMMA-based transfer method. Evidence for contamination effects is given in Fig. 4b, thus pore size fabrication is limited to just below 10 nm.

2.2.3. Hexagonal boron nitride flakes

Hexagonal boron nitride (h-BN) is an insulating isomorph of graphite that consists of boron and nitrogen atoms occupying the sites of the two triangular sublattices. Within each layer of h-BN, boron and nitrogen atoms are bound by strong covalent bonds, whereas the layers are held together by weak Van der Waals forces, as in graphite. Therefore, h-BN films can be exfoliated from bulk BN crystals by micromechanical cleavage. We used h-BN platelets, with sizes of several microns, produced by exfoliation of a commercially available high quality h-BN powder [21] and transferred to precise positions using the wedging method described earlier.

Nanopores in h-BN were fabricated on the highly transparent flakes with pore sizes as small as 8 nm (Fig. 5). We noticed important differences when comparing h-BN with graphene flakes with respect to the resistance to ion irradiation and found that the h-BN flakes peel off even at moderate imaging doses [22–24]. With

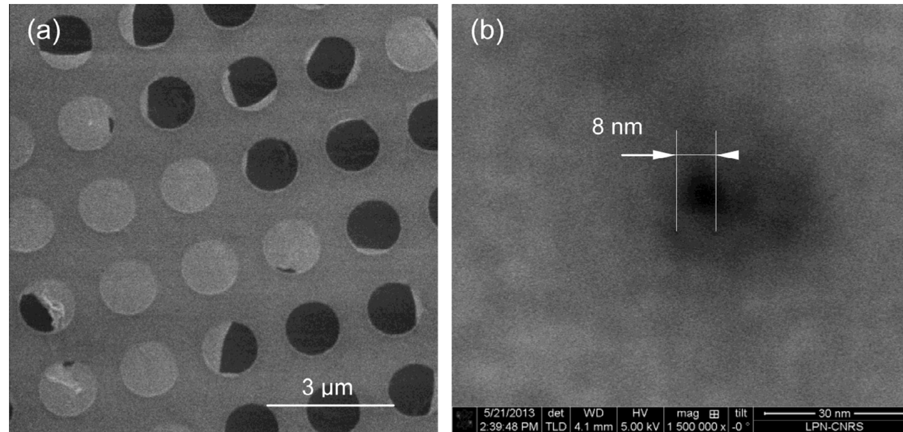

Fig. 3. (a) Graphene flakes mechanically exfoliated and micro-positioned onto holey films or FIB patterned micro-sized pores. (b) SEM image of an 8 nm drilled pore in a graphene flake consisting of about three atomic monolayers 5×10^4 ions/pt.

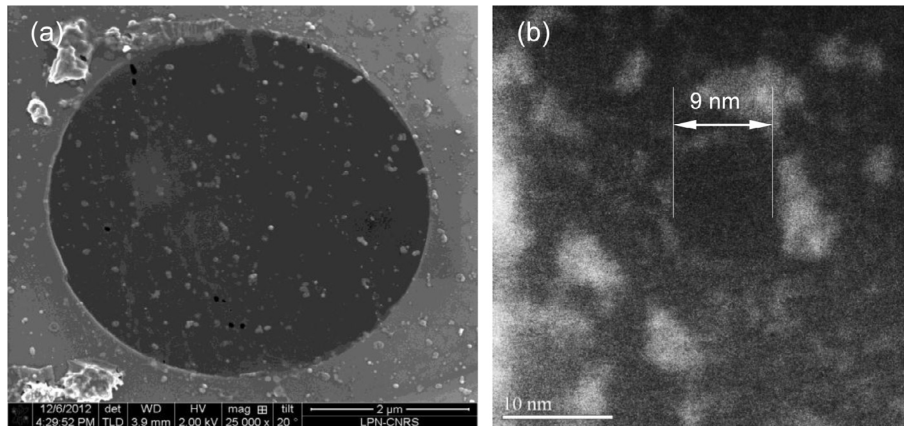

Fig. 4. (a) Graphene CVD grown film transferred onto 2 µm holes patterned by FIB. (b) SEM image of a 9 nm drilled pore on a graphene sheet of a few atomic monolayers 8.25×10^4 ions/pt.

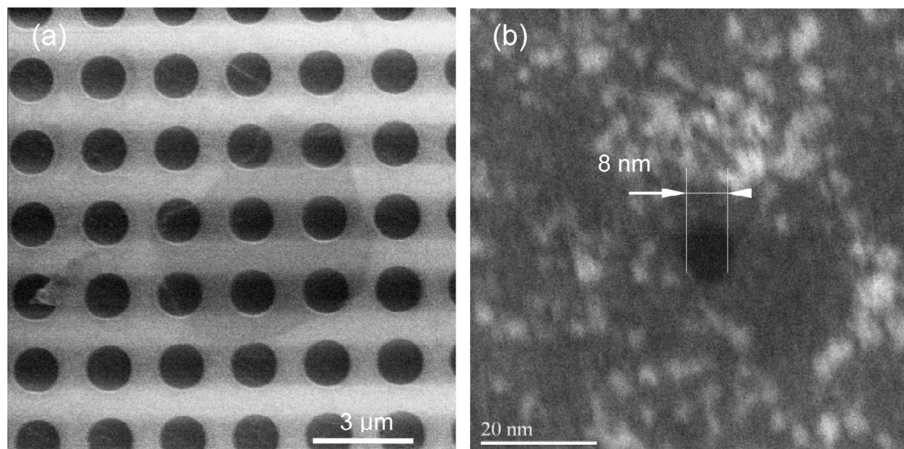

Fig. 5. (a) FIB image in the Ion Microscopy mode showing the high transparency of the h-BN flake consisting of three atomic monolayers. (b) STEM image of a nanopore in a three atomic monolayer h-BN flake. Pore size diameter 8 nm at 6.75×10^4 ions/pt. Surface contamination was observed and identified as hydrocarbon-based.

respect to electrical conductivity no charging effects were noticed apart from the peeling effects mentioned above. Thus the focus and probe shaping sequences must be kept very short. Surprisingly the dwell times for engraving nanopores do not differ significantly between graphene and h-BN flakes (Table 1).

During our experimentations and observations, we have also checked for the presence of gallium ions in the vicinity of the h-BN drilled pores. The resulting analysis, in Fig. 6, shows that there is no trace of gallium ions and the h-BN crystal structure remains preserved as our previous results suggested [17]. Our

Table 1
Summary of the nanopore engraving process on different materials and thicknesses using 30 kV Ga^+ ions.

Material	Thickness	Ø Hole (nm)	Doses (ions/pt)
SiC	100 nm	110	4.4×10^7
SiN	30 nm	~100	4.7×10^5
SiO_2	20 nm	8	3×10^5
h-BN	Few layers	8	6.75×10^4
Graphene	HOPG	7.8	5.00×10^4
	CVD	9.2	8.25×10^4

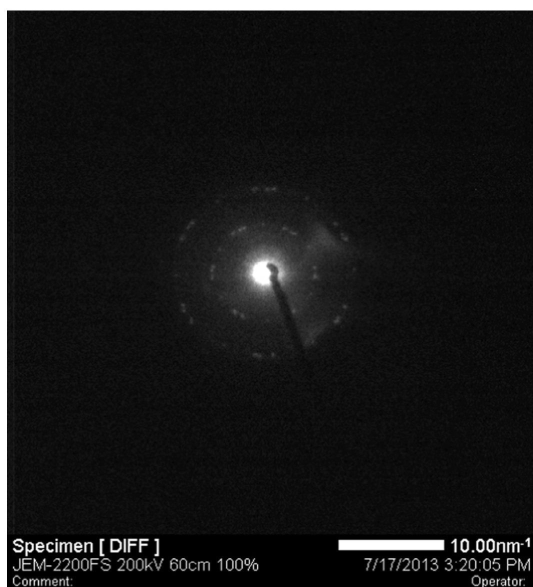

Fig. 6. TEM diffraction pattern observed in the vicinity of a nanopore drilled in a few layer h-BN flake. This analysis shows that there is no trace of gallium ions and the h-BN crystal structure remains preserved.

interpretation is that the interaction of a membrane having only a few atoms in thickness with an energetic gallium ion (30–35 keV) leads to a single collision process, that stops once the ion has traversed the sheet. Therefore, only a fraction of the gallium ion energy can be transferred to the 2D crystalline system and this avoid membrane contamination by the incoming gallium ions.

3. Conclusions and perspectives

We have demonstrated that finely focused pencils of gallium ions allow for the reproducible fabrication, as well as the customization, of nanopore-based devices that can be defined in the sub-10 nm range. The combination of a precise placement and of short engraving times, typically in the millisecond range, makes it compatible with batch processing and allows for small series of devices to be patterned in a tailored manner.

The methodology for preparation, manipulation and transfer that we have described allowed robust, free-standing and atomically-thin sheets of both graphene and h-BN to be obtained and positioned on a variety of support media. Such samples can be considered as ideal templates for exploring the limits of gallium-FIB patterning.

An important and unexpected finding of this study is that, in contrast to gallium-FIB engraving of dielectric or metallized silicon-based membranes, nanopores patterned in atomically thin sheets of graphene or h-BN have sizes that appear to be limited to around 8 nm. These materials exhibit unusual properties:

– High transparency. Atomically-thin flakes allow an important fraction of the incident gallium beam to be transmitted, generating a high secondary electron signal when impacting the sample holder metal surface.
– h-BN flakes are easily destroyed during imaging when the beam is digitally scanned over μm-sized area with only a few ions per point, but drilling a single nanopore in the same material require 10 millions of ions directed to a single pixel to produce a stable nanopore. This can be the result of the insulating properties of h-BN.
– We have verified that for atomically thin flakes of both graphene and h-BN the fabricated pores do not exhibit circular shapes for diameters below 10–15 nm.

These observations suggest that reconstruction effects may occur and that a gallium ion dose threshold has to be deposited in order to pattern stable nanopores. Below a critical deposited dose, we were unable to observe any open circular nanopores in both graphene and h-BN atomically thin sheets. This effect has been already predicted using molecular dynamics simulations [23,24] and is currently under investigation in our team. In the light of our investigations nanopores were carved in such h-BN flakes using a dedicated gallium FIB nanowriter and this material appears very promising for biosensing applications.

Acknowledgment

This work was partially supported by the ANR "BioGraph'N" and "MIKADO" research projects.

References

[1] M. Henini, III–Vs Review 12 (6) (1999) 18–23.
[2] L. Pain, S. Tedesco, C. Constancias, C. R. Phys. 7 (2006) 910–923.
[3] S. Reyntjens, R. Puers, J. Micromech. Microeng. 11 (2001) 287–300.
[4] B. Schiedt et al., Microelectron. Eng. 87 (5–8) (2010) 1300–1303.
[5] See e.g. <http://www.norcada.com/>, <http://www.nanoporesolutions.com/>.
[6] A.J. Storm et al., Nat. Mater. 2 (2003) 537–540.
[7] M. van den Hout, C. Dekker, et al., Nanotechnology 21 (2010) 115304.
[8] J. Yang, A.R. Hall, et al., Nanotechnology 22 (2011) 285310.
[9] A.T. Kuan, J.A. Golovchenko, Appl. Phys. Lett. 100 (2012) 213104.
[10] N. Patterson et al., Nanotechnology 19 (2008) 23530–23533.
[11] A. Weidinger, Europhys. News 35 (5) (2004) p153–p155.
[12] J. Gierak, R. Jede, P. Hawkes, Nanolithography with focused ion beams, in: S. Cabrini, S. Kawata (Eds.), Nanofabrication Handbook, CRC Press, 2012. see also: <ftp://ftp.cordis.europa.eu/pub/nanotechnology/docs/n_s_nanofib_27052002.pdf>.
[13] J. Gierak et al., Microelectron. Eng. 84 (5–8) (2007) 779–783.
[14] A.-L. Biance, J. Gierak, Microelectron. Eng. 83 (4–9) (2006) 1474–1477.
[15] A.K. Geim, Science 324 (2009) 1530–1534.
[16] S. Garaj, W. Hubbard, et al., Nature 467 (2010) 190–193.
[17] A. Morin, D. Lucot, et al., Microelectron. Eng. 97 (2012) 311–316.
[18] J. Li et al., Nature 412 (2001) 166–169.
[19] J. Gierak, Semicond. Sci. Technol. 24 (4) (2009) 043001.
[20] Oxford instrument Agar Quantifoil 1.2 μm dia, separation 1.3 μm.
[21] St Gobain Advanced Ceramics Boron Nitride Products, <www.TRESBN.com>.
[22] O. Lehtinen, E. Dumur, et al., Nucl. Instrum. Methods B 269 (2011) 1327–1331.
[23] W. Li, L. Liang, S. Zhao, S. Zhang, J. Xue, J. Appl. Phys. 114 (2013) 234304.
[24] J. Kotakoski, O.J. Lehtinen, MRS Proc. 1259E (2010). pp. 1259-S18-02.